How Dimensionality Affects the Structural Anomaly in a Core-Softened Collo

Leandro B. Krott [‡] and José Rafael Bordin [*,‡]

Posted Date: 21 February 2023

doi: 10.20944/preprints202302.0349.v1

Keywords: Confined colloids; waterlike anomalies; Molecular Dynamics simulation

Article

How Dimensionality Affects the Structural Anomaly in a Core-Softened Colloid

Leandro B. Krott [1,†] and José R. Bordin [2,*,†]

[1] Centro de Ciências, Tecnologias e Saúde, Campus Araranguá, Universidade Federal de Santa Catarina, Rua Pedro João Pereira, 150, CEP 88905-120, Araranguá, SC, Brazil.; leandro.krott@ufsc.br

[2] Departamento de Física, Instituto de Física e Matemática, Universidade Federal de Pelotas. Caixa Postal 354, CEP 96001-970, Pelotas, RS, Brazil; jrbordin@ufpel.edu.br

* Correspondence: jrbordin@ufpel.edu.br

† These authors contributed equally to this work.

Abstract: The interaction between hard-core soft-shell colloids are characterized by having two characteristic distances: one associated with the penetrable, soft corona and another one corresponding to the impenetrable core. Isotropic core-softened potentials with two characteristic length scales have long been applied to understand the properties of such colloids. Those potentials usually show waterlike anomalies, and recent findings have indicated the existence of multiple anomalous regions in the 2D limit under compression, while in 3D only one anomalous region is observed. In this direction, we perform Molecular Dynamics simulations to unveil the details about the structural behavior in the quasi-2D limit of a core-softened colloid. The fluid was confined between highly repulsive solvophobic walls, and the behavior at distinct wall separation and colloid density was analyzed. Our results indicated a straight relation between the 2D or 3D-like behavior and the layers separation. We can relate that if the system behaves as independent 2D-layers, it will have a 2D-like behavior. However, for some separations the layers are connected, with colloids hopping from one layer to another – having then a 3D-like structural behavior. Those findings fill the gap in the depiction of the anomalous behavior from 2D to 3D.

Keywords: confined colloids; waterlike anomalies; molecular dynamics simulation

1. Introduction

There are a large number of models for fluids and colloids, ranging from *ab initio* and atomistic molecular dynamics simulations to continuum models. In between this extrema, symmetric core-softened (CS) potentials are a class of effective models largely employed to study competitive systems, where the two characteristic length scales in the effective interaction between the particles try to dominate the fluid structure [1]. Usually, colloids are made of molecular subunits which form a central packed agglomeration and a less dense, more entropic peripheral area. With these, colloidal particles show distinct conformations that compete to rule the suspension behavior [2]. In this sense, they are usually modeled using isotropic CS potentials [3,4].

Although isotropic, the CS class of potentials shows a competition that come from the existence of two characteristic length scales in the potential [5–14] or from softened repulsive potentials [15–19]. As examples, experimental works have shown that the effective interaction in solutions of pure or grafted PEG colloids and Ficoll are well described by two length scales potentials [20–24]. Likewise, computational studies indicate the same type of effective interactions for polymer-grafted nanoparticles [25,26] or star polymers [27].

Water, the most common solvent for colloidal suspensions and the most important material in Earth, also shows a competition between two structures that originates from the hydrogen bonds breaking and forming between the water molecules [28–30]. As a consequence, water shows more than 70 anomalous behaviors due this struggle between two conformations trying to dominate the fluid structure [31]. Anomalies are properties that differ from the expected and observed in most materials.

 doi:10.20944/preprints202302.0349.v1

Certainly, the most well known water anomaly is the density anomaly: normal liquids contract upon cooling at constant pressure, while anomalous fluids expand as the temperature decreases. This anomaly leads to the maximum value in the water density, $1 g/cm^3$ at 4^oC and constant pressure of 1 atm [32]. Also, anomalous fluids get disordered as the density increases – the opposite from the expected: a higher order in the system as the density grows [33]. In this sense, CS potentials are simple effective models that allow us to unveil the mechanisms behind the behavior of complex fluids as water and hard core - soft shell colloidal suspensions [34–48].

The shape and the type of interaction between colloidal particles combined with the presence of distinct confining surfaces have key roles in self-assembly, phase separation, interfacial activities and anomalous behavior of systems modeled by CS potentials [49–53]. Those peculiarities are in agreement with several experiments involving colloidal cluster, formation of self-assembled mesophases, layering packing and synthesis of new structures using amphiphilic molecules [54–59].

Additionally, structure of colloidal systems has been extensively studied by molecular dynamics and Monte Carlo simulations and the presence of patterns have been found for 3D bulk [42], 2D bulk [60–62] and confined systems [52,63–71]. Significant differences are reported when going from a 2D to a quasi-2D system. When confined in very small slit pores, CS potentials can present a 2D-like behavior, but growing the size of slit pores affects the solid-liquid transition at low densities due the out-of-plane motion of particles [71]. Likewise, the quasi-2D limit can affect the temperature of maximum density observed in CS models [72] and the crystalline structure [73].

Specifically, de Oliveira and co-authors proposed a CS ramp-like potential that presents thermodynamic, dynamic and structural anomalies obeying the same hierarchy observed in water [74,75]. Since then, effects of hydrophobic and hydrophilic confinement through plates and nanotubes on those anomalies and in solid-liquid and surface transitions also have been studied [76–79]. They show that entropic effect from flexibility of confining walls can break the dynamic and structural anomalies of the CS fluid [80], as well induce superdiffusive to diffusive first order phase transition [81]. On the other hand, rigid walls can induce surface phase transitions [82] and arise a new region of structural anomaly [83]. More recently, Bordin and Barbosa [84] studied the 2D case of this CS fluid. They found a second region of density, diffusion and structural anomaly at high densities. The first region of anomalies is associated with the competition between scales of CS potential, while the second one is generated by a reentrant fluid marking an order-disorder transition. Besides that, an inversion of hierarchy on these anomalies was observed, in agreement with results from Dudalov et. al [85]. Later, Cardoso and co-workers [62] found a third region of structural anomaly at higher densities. They show that each anomalous behavior can be associated to reentrant fluid phases that separates two solid crystalline regions, and to distinct aggregates size in the fluid phase.

But where is the boundary between the 3D behavior, with one region of structural anomaly in the fluid phase associated to a crystalline-amorphous solid transition [75,86] and the 2D behavior, where up to three anomalous structural regions was found [49,62]? To unveil this location, we expand our previous works [64,82,83] to see what happens in the quasi-2D limit with the CS model confined between two flat, highly repulsive solvophobic walls. Our findings indicate that the limit between 2D-like or 3D-like behavior is associated to the layering and with the existence of order-disorder transitions in the layers.

This paper is organized as follow: in section 2, we present the model; in section 3, we present the methods and simulation details; in section 4, we discuss the results; and, in section 5, we present the conclusions.

Preprints (www.preprints.org) | NOT PEER-REVIEWED | Posted: 21 February 2023 doi:10.20944/preprints202302.0349.v1

2. The Model

The colloidal system is modeled by spherical particles confined between smooth parallel plates. The particle-particle (P-P) interaction occurs through a two length scales potential, given by

$$\frac{U(r_{ij})}{\varepsilon} = 4\left[\left(\frac{\sigma}{r_{ij}}\right)^{12} - \left(\frac{\sigma}{r_{ij}}\right)^{6}\right] + a\exp\left[-\frac{1}{c^2}\left(\frac{r_{ij}-r_0}{\sigma}\right)^2\right] \tag{1}$$

where $r_{ij} = |\vec{r}_i - \vec{r}_j|$ is the distance between two particles, i and j. The first term is a standard Lennard-Jones (LJ) 12-6 potential where ε is the depth and σ the particle's diameter. The second one is a gaussian centered on radius r_0 and width c. We used the following parameters: $a = 5$, $r_0/\sigma = 0.7$ and $c = 1$, that reproduces waterlike anomalies, like density, diffusion and structural anomalies [74,75]. The P-P interaction potential has a cutoff of $r_c/\sigma = 3.5$.

The wall-particle (W-P) interaction is given by a strong repulsive potential, the so-called R6 potential [79,83]

$$U_{R6}(z) = \begin{cases} 4\varepsilon(\sigma/z)^6 + 0.1875\varepsilon(z/\sigma) - U_{R6c}, & z \le z_c \\ 0, & z > z_c \end{cases} \tag{2}$$

where z is the distance between the particles and the walls, $z_c = 2.0\sigma$ and $U_{R6c} = 4\varepsilon(\sigma/z_c)^6 + 0.1875\varepsilon(z_c/\sigma)$. Figure 1 shows the profile of P-P and W-P interaction potentials. All quantities used in this work are given in LJ units [87], like for example, distance $r^* = r/\sigma$ and temperature $T^* = k_BT/\varepsilon$. The symbol * will be omitted for simplicity.

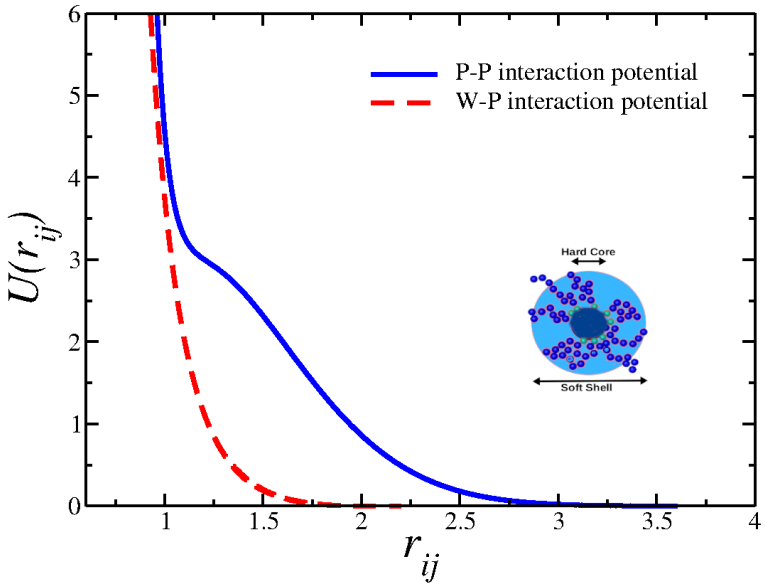

Figure 1. Particle-particle (P-P) interaction potential (solid blue line) and wall-particle (W-P) interaction potential (dashed red line). Insert show the schematic depiction of a hard core-soft shell polymer coated nanoparticle as a core-softened effective colloid [25].

3. Methods and Simulation Details

We perform molecular dynamics simulations in the NVT ensemble. 2028 particles were confined between two parallel smooth fixed plates. The walls are held fixed in the z direction and separated by a distance L_z. L_z was varied from 4.8 to 6.2. Those specific separations were chosen so we can study system with two or three particles layers. For each fixed L_z, we change the simulation box size, given by L, in order to simulate different total densities. Total densities are defined as $\rho = N/(L_{ze}L^2)$, where $L_{ze} = L_z - \sigma$ is the effective distance between the plates. Periodic boundary conditions were used in x

Preprints (www.preprints.org) | NOT PEER-REVIEWED | Posted: 21 February 2023 doi:10.20944/preprints202302.0349.v1

and y directions. Our simulations were performed along the isotherm $T = 0.150$ and we analyzed the effects of varying ρ and L_z.

The equations of motion were integrated through Velocity Verlet algorithm, and the Nose-Hoover heat-bath with a coupling parameter Q = 2 was used to kept T fixed. Equilibration was reached after 2×10^6 time steps of simulation and followed by 1×10^6 time steps for the production of results. The time step was $\delta t = 0.001$, and to ensure the equilibration, we track the lateral pressure and energy as function of time.

The system structure was analysed by the transversal density profile and the lateral radial distribution function, besides some correlated quantities, like translational order parameter, the two-body entropy and the cumulative two-body entropy. The lateral radial distribution function $g_{\parallel}(r_{\parallel})$ is defined as

$$g_{\parallel}(r_{\parallel}) \equiv \frac{1}{\rho^2 V} \sum_{i \neq j} \delta(r_{\parallel} - r_{ij}) \left[\theta\left(|z_i - z_j|\right) - \theta\left(|z_i - z_j| - \delta z\right)\right]. \tag{3}$$

where $r_{\parallel}$ is the parallel distance between particles in the x and y directions. Considering that systems structure themselves in layers, the Heaviside function, $\theta(x)$, restricts the sum of particle pairs in the same slab of thickness $\delta z/\sigma = 1.0$ for contact and central layers.

The translational order parameter is defined as [88–90]

$$\tau = \int \mid g(\epsilon) - 1 \mid d\epsilon, \tag{4}$$

where $\epsilon = r_{\parallel}\rho_l^{1/2}$. We calculate the average number of particles per layer, $< N_l >$, and define the layer density as $\rho_l =< N_l > /(L^2 \delta z)$.

The translational order parameter provides us information about the structure of the system. Gas and liquids have low values of τ, while crystal and amorphous solids present high values of τ. In normal fluids, τ increases monotonically with density or pressure at constant temperature, but in anomalous fluids τ decreases with density or pressure for some temperatures. The current potential presents one region of anomaly in the 3D bulk system [75], due the competition between scales. For confined systems and considering the particles near to the walls (contact layers), besides the anomalous region due the competition between scales, another one rises induced by nanoconfinement at low densities [83]. More recent works [62,84] showed that dimensionality leads to extra structural anomalies at higher densities and low temperatures.

The two-body entropy is a structural quantity. It is defined as [91]

$$s_2 = -\frac{\rho_l}{2} \int \left[g_{\parallel}(r_{\parallel}) \ln(g_{\parallel}(r_{\parallel})) - g_{\parallel}(r_{\parallel}) + 1\right] d^2 r_{\parallel}, \tag{5}$$

The normal behavior of s_2 is to decrease with density or pressure at constant temperature. However, in anomalous systems s_2 increases with the density or pressure at some region of its phase diagrams - the anomalous region. Like the translational order parameter, s_2 also presented a double region of anomaly for confined systems [83] and a triple anomalous region for the 2D case [62].

The last quantity analyzed was the cumulative two-body entropy, defined as [92]

$$C_{s2}(R) = -\pi \int_0^R \left[g_{\parallel}(r_{\parallel}) \ln(g_{\parallel}(r_{\parallel})) - g_{\parallel}(r_{\parallel}) + 1\right] r_{\parallel} dr_{\parallel}, \tag{6}$$

where R is the upper integration limit. This quantity give us information about the long range translational order. For fluids and amorphous phases, that do not present long range information, $C_{s2}(R)$ converges, while for solids, that present long range information, $C_{s2}(R)$ diverges.

Preprints (www.preprints.org) | NOT PEER-REVIEWED | Posted: 21 February 2023 doi:10.20944/preprints202302.0349.v1

4. Results

We can imagine the 2D limit as the single layer limit. In this sense, we have investigated systems with two, two-to-three or three layers of confined CS colloids, depicted by their transversal density profiles in Figure 2(a). Layers near to the walls are called contact layers, while the others, if exist, are called central layers. Systems with two well defined layers are observed for the most densities explored for plates separated by $L_z = 4.8$ and 5.0, while three well defined layers occur for $L_z = 5.8$ to 6.2. Intermediate values of L_z lean over to present a transition between two-to-three layers for most densities simulated. In Figures 2(b) and (c) we show examples of snapshots of systems with two ($L_z = 4.8$) and three ($L_z = 6.0$) well defined layers, respectively.

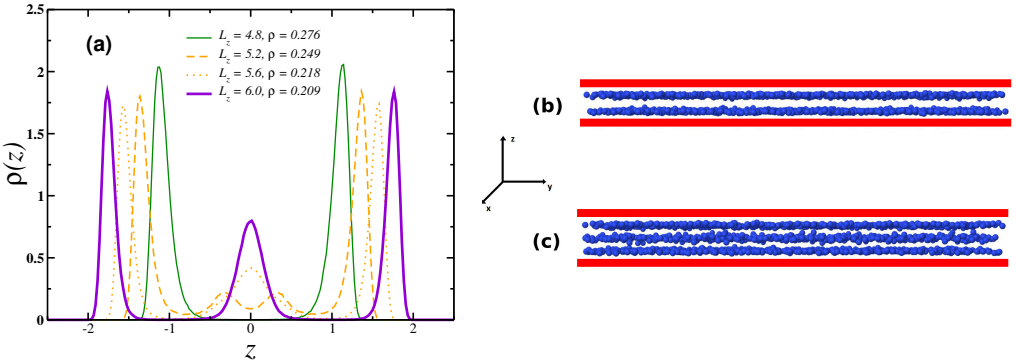

Figure 2. (a) Transversal density profile for some systems that present formation of two (green solid line), two-to-three (orange dashed and dotted lines) and three layers (violet solid line) of particles between plates. Examples of snapshots of systems with **(b)** two layers for plates separated by $L_z = 4.8$ and **(c)** three layers for plates separated by $L_z = 6.0$. The fluid particles are in blue and the confining walls are in red.

Our first analysis is related to particles located near to the walls, the contact layers. As already mentioned, this model has one region of anomaly in translational order parameter, τ, for 3D bulk system [75,86] due the competition between scales and three regions of anomaly for 2D bulk system [84], two of them due the competition between sales and another one due the order-disorder transition at intermediary ($\rho \approx 0.42$) and high ($\rho \approx 0.65$) densities [62]. Confining fixed walls also induce a new region of anomaly at low densities, $\rho_l < 0.350$ [83]. Now, we present the behavior of τ for higher densities that studied in the past and we found the peculiar profile presented in Figure 3(a). It shows the parameter τ for the contact layer as function of layer density, ρ_l, for several separation of plates at $T = 0.150$. Systems with plates separated by $L_z = 5.2$, 5.3, 5.5 and 5.6, drafted in orange lines, do not have anomaly for $\rho_l \approx 0.400$, that is, present a 3D-like fluid (or disordered) behavior. On the other hand, the another curves corresponding to $L_z = 4.8$, 5.0, 5.8, 6.0 and 6.2, present a third region of anomaly, what means a 2D-like (ordered) behavior for this gap of densities ($0.400 \leq \rho_l \leq 0.500$), including the same values of ρ_l comparing to found for 2D systems [62,84].

Another quantity analyzed was the two-body entropy, that gives us structural information, because its definition is based on the radial distribution function (equation 5). Normal fluids lean over to present values of s_2 that monotonically decrease with density. s_2 also presents anomalous behavior in 3D and 2D bulk and 3D confined systems. Two regions of anomaly in s_2 were already shown in the past for ρ_l until ≈ 0.350. Now, going to higher layer densities, we found the profile seen in Figure 3(b). In current work we explore higher densities and we found a 2D-like and a 3D-like behavior, depending on the L_z studied. Like observed for the translational order parameter, s_2 also presented a 2D-like behavior at high densities ($0.400 \leq \rho_l \leq 0.500$) for $L_z = 4.8$, 5.0, 5.8, 6.0 and 6.2 and a 3D-like behavior for $L_z = 5.2$, 5.3, 5.5 and 5.6.

Preprints (www.preprints.org) | NOT PEER-REVIEWED | Posted: 21 February 2023 doi:10.20944/preprints202302.0349.v1

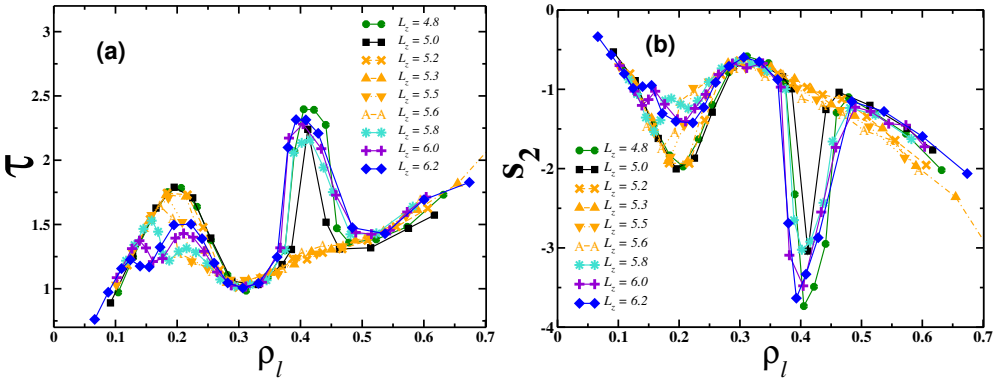

Figure 3. (a) Translational order parameter τ and **(b)** two-body entropy s_2 as function of layer density ρ_l at different separations of plates (L_z) and $T = 0.150$. Both quantities are related to contact layers.

To understand why some cases have one or more structural anomalous regions, and their origins, we analyze the transversal density profile ($\rho(z) \times z$), the lateral radial distribution function ($g(r_{||}) \times r_{||}$) and the cumulative two-body entropy ($|C_2(r_{||})| \times r_{||}$) for three situations: the lowest separation $L_z = 4.8$, corresponding to a system that present two layers, the separation $L_z = 6.0$ that present three layers and a intermediate case, $L_z = 5.5$, that has a two-to-three layers transition.

Let's begin by analyzing the data for $L_z = 4.8$, Figure 4. The solid green lines correspond to densities in the region of highly-ordered particles, $0.390 \leq \rho_l \leq 0.441$. The dashed light green lines correspond to some immediately densities above the maximum in τ and minimum in s_2, while the dashed-dotted light green lines correspond to some immediately densities below the maximum in τ and minimum in s_2. In Figure 4(a), the transversal density profiles show two well defined layers, evidenced by zoom given in the inset graph, which suggests ordered particles. The Figure 4(b) shows the lateral radial distribution function and makes evident the ordering of particles in the third maximum of τ (solid green lines) comparing to vicinity densities (disorder-order-disorder transition), the same behavior observed in 2D system [62,84]. The long range translational behavior, given by the cumulative two-body entropy, $|C_2(r_{||})|$, confirms the tendency of solidification at densities $0.390 \leq \rho_l \leq 0.441$.

The same behavior was found for another system that present 2D-like behavior at high densities, $L_z = 6.0$, shown in Figure 5. The solid violet lines correspond to densities in the region of ordered particles (third maximum in τ and minimum in s_2), $0.381 \leq \rho_l \leq 0.458$. The dashed magenta lines correspond to some densities immediately above the maximum in τ and minimum in s_2, while the dashed-dotted magenta lines correspond to some densities immediately below the maximum in τ and minimum in s_2. Although the fact that here the colloids are arranged in three well defined layers, like seen in Figure 5(a) and its inset graph, the basic mechanism behind the structural anomalous region is the same as the one found for the previous case, Figure 4. Both $g(r_{||})$ and $|C_2(r_{||})|$ indicate a order-disorder transition in the contact layers, as we can see in Figure 5(b) and (c), respectively. Therefore, the origin is the same as the one observed in the 2D system: a ordered-disordered transition leads to the waterlike structural anomaly.

Preprints (www.preprints.org) | NOT PEER-REVIEWED | Posted: 21 February 2023 doi:10.20944/preprints202302.0349.v1

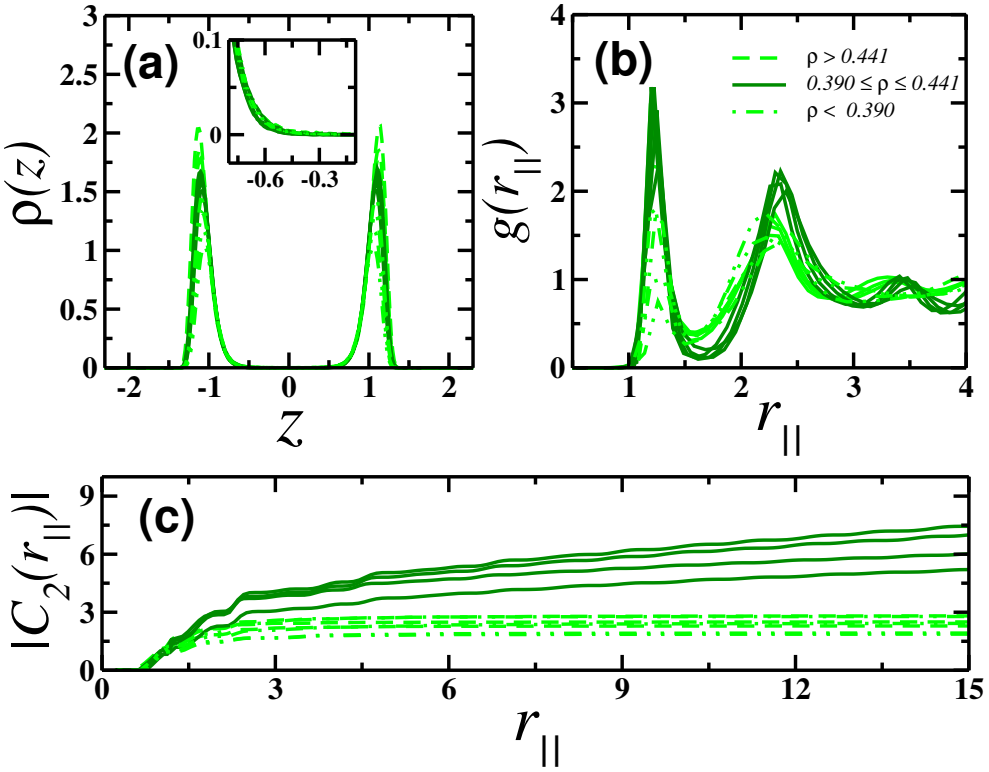

Figure 4. Quantities related to $L_z = 4.8$ at $T = 0.150$: **(a)** transversal density profile, **(b)** lateral radial distribution function and **(c)** cumulative two-body entropy.

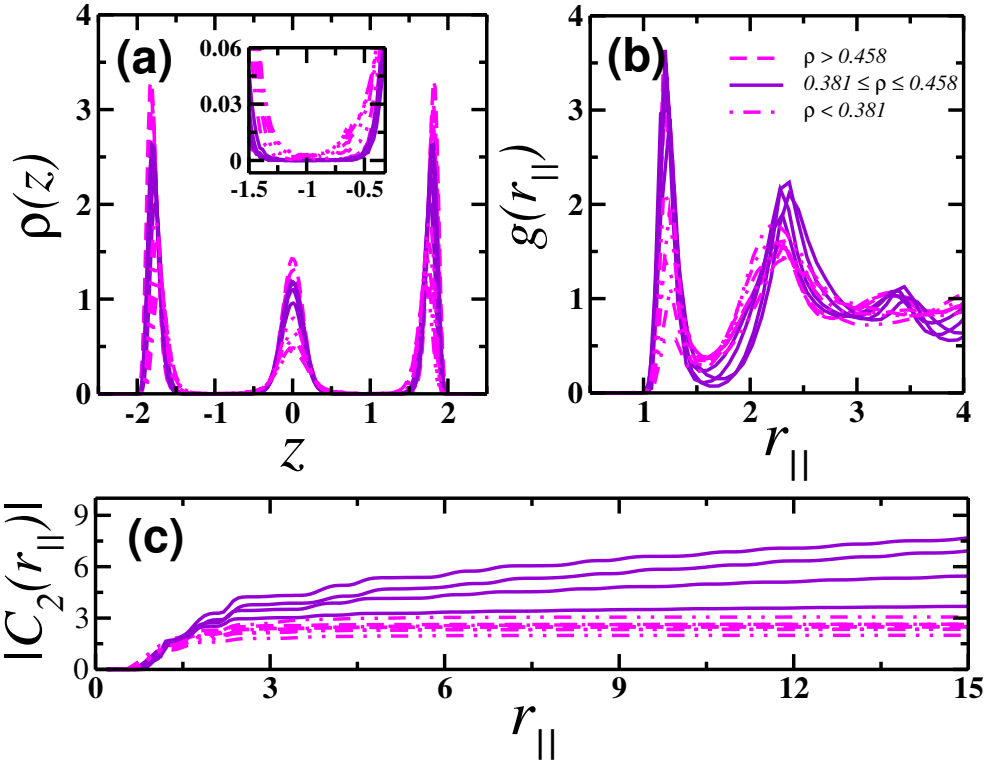

Figure 5. Quantities related to $L_z = 6.0$ at $T = 0.150$: **(a)** transversal density profile, **(b)** lateral radial distribution function and **(c)** cumulative two-body entropy.

So far, we have observed a 2D-like behavior and mechanism for the structural anomalies in systems with two and three layers. But what happens in systems with a single anomalous region? To

Preprints (www.preprints.org) | NOT PEER-REVIEWED | Posted: 21 February 2023 doi:10.20944/preprints202302.0349.v1

clarify this point, we show in Figure 6 the $L_z = 5.5$ case. The solid orange lines correspond to densities in the region that should present ordered particles (third maximum in τ and minimum in s_2 for another cases), $0.394 \leq \rho_l \leq 0.465$. The dashed yellow lines correspond to densities slightly above, while the dashed-dotted yellow lines correspond to densities slightly below the region where it was supposed to happen the ordering of particles. In Figure 6(a), the transversal density profiles show a two-to-three layers transition. However, as indicated by the zoom in the inset graph, the density does not go to zero in the region between the layers. Unlike the previous cases (Figures 4 and 5), here there is a connection between contact and central layers. This indicates that some particles from the central layer jump to the contact layer, and the other way around as well. This is a consequence of the frustration added by this specific separation length, that forces the colloids to organize themselves in such way that the separation between two layers is smaller than the second length scale in the CS potential but bigger than the first length scale. This frustration prevents the system to relax to an organized phase. It is clear also in Figure 6(b). The lateral radial distribution function does not go to zero for separations between the first and second peaks, preventing the ordered phase. This is corroborated by the cumulative two-body entropy, $|C_2(r_{||})|$, that presents a liquid (disordered) profile for all densities, like shown in Figure 6(c). Without order-disorder transition, the system leans to present a 3D-like behavior.

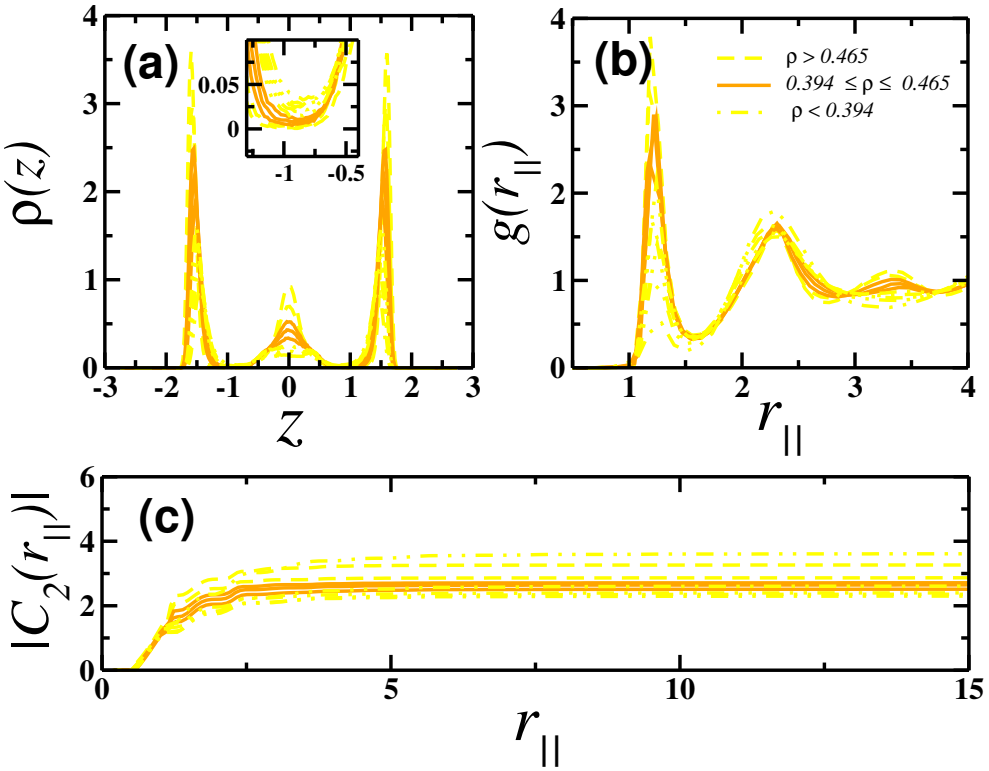

Figure 6. Quantities related to $L_z = 5.5$ at $T = 0.150$: **(a)** transversal density profile, **(b)** lateral radial distribution function and **(c)** cumulative two-body entropy.

Preprints (www.preprints.org) | NOT PEER-REVIEWED | Posted: 21 February 2023 doi:10.20944/preprints202302.0349.v1

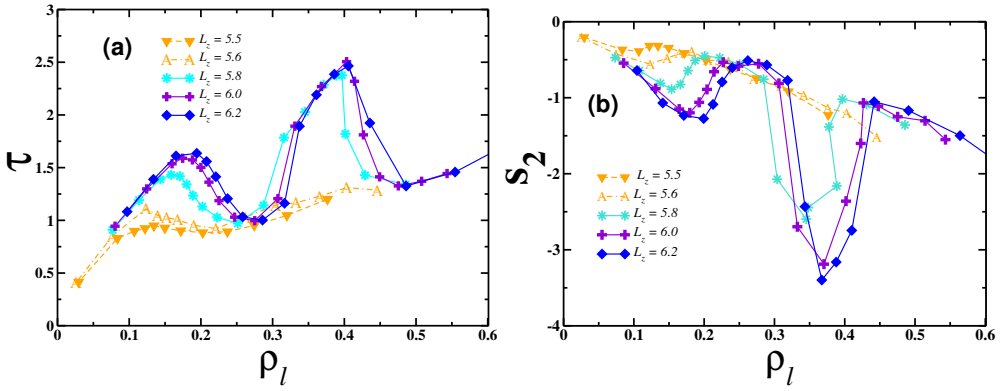

Figure 7. **(a)** Translational order parameter and **(b)** two-body entropy as function of central layer density. The central layers were analyzed at $T = 0.150$.

The central layer was observed for separations in the range $5.5 \leq L_z \leq 6.2$. For these separations, the anomalous regions at high densities (around ≈ 0.4) can be observed in the central layer for the cases the three layers are well defined - without particles hopping from one layer to another one.

5. Conclusions

Core-softened colloids can have unique and peculiar structural properties. The model employed in this study shows multiple regions of structural anomalous behavior in 2D, while the 3D case has only one. Our quest in this paper was to unveil the details about the structure of a CS model in the quasi-2D limit.

Our findings indicate the limit between 2D and 3D-like structural behavior for confined colloids: if the CS particles layers can accommodate themselves near one of the characteristic interaction length scales, the layers act as independent 2D systems – colloids from one layer do not jump to another one. On the other hand, if the confinement frustrates the system, does not allowing a inter-layer separation close to one of the potential length scale, the colloids move from one layer to another, no longer acting as independent layers, but approaching the 3D limit by having this translational hopping between the layers.

Funding: Without public funding this research would be impossible. JRB is grateful to the CNPq, proc. 304958/2022-0, and FAPERGS, TO 21/2551-0002024-5, for the funding support.

Data Availability Statement: All data is available upon reasonable request.

Conflicts of Interest: The authors declare no conflict of interest.

References

1. Vilaseca, P.; Franzese, G. Isotropic soft-core potentials with two characteristic length scales and anomalous behaviour. *Journal of Non-Crystalline Solids* **2011**, *357*, 419 – 426. 6th International Discussion Meeting on Relaxation in Complex Systems, doi:https://doi.org/10.1016/j.jnoncrysol.2010.07.053.
2. Ruiz-Franco, J.; Zaccarelli, E. On the Role of Competing Interactions in Charged Colloids with Short-Range Attraction. *Annual Review of Condensed Matter Physics* **2021**, *12*, 51–70. doi:10.1146/annurev-conmatphys-061020-053046.
3. Shukla, A.; Mylonas, E.; Di Cola, E.; Finet, S.; Timmins, P.; Narayanan, T.; Svergun, D.I. Absence of equilibrium cluster phase in concentrated lysozyme solutions. *Proceedings of the National Academy of Sciences* **2008**, *105*, 5075–5080.
4. Yethiraj, A. Tunable colloids: control of colloidal phase transitions with tunable interactions. *Soft Matter* **2007**, *3*, 1099.
5. Jagla, E.A. Phase behavior of a system of particles with core collapse. *Physical Review E* **1998**, *58*, 1478.
6. Jagla, E.A. Minimum energy configurations of repelling particles in two dimensions. *Journal of Chemical Physics* **1999**, *110*, 451.

7. Jagla, E.A. Core-softened potentials and the anomalous properties of water. *Journal of Chemical Physics* **1999**, *111*, 8980.
8. de Oliveira, A.B.; Netz, P.A.; Barbosa, M.C. Interplay between structure and density anomaly for an isotropic core-softened ramp-like potential. *Physica A* **2007**, *386*, 744–747.
9. Barbosa, M.A.; Salcedo, E.; Barbosa, M.C. Multiple liquid-liquid critical points and density anomaly in core-softened potentials. *Physical Review E* **2013**, *87*, 032303.
10. Fomin, Y.D.; Tsiok, E.N.; Ryzhov, V.N. Inversion of sequence of diffusion and density anomalies in core-softened systems. *Journal of Chemical Physics* **2011**, *135*, 234502.
11. Yan, Z.; Buldyrev, S.V.; Giovambattista, N.; Stanley, H.E. Structural Order for One-Scale and Two-Scale Potentials. *Physical Review Letters* **2005**, *95*, 130604.
12. Fomin, D.Y.; .; Gribova, N.V.; Ryzhov, V.N.; Stishov, S.M.; Frenkel, D. Quasibinary amorphous phase in a three-dimensional system of particles with repulsive-shoulder interactions. *Journal of Chemical Physics* **2008**, *129*, 064512.
13. Lascaris, E.; Malescio, G.; Buldyrev, S.V.; Stanley, H.E. Cluster formation, waterlike anomalies, and re-entrant melting for a family of bounded repulsive interaction potentials. *Physical Review E* **2010**, *81*, 031201.
14. Buldyrev, S.V.; Malescio, G.; Angell, C.A.; Giovambattista, N.; Prestipino, S.; Saija, F.; Stanley, H.E.; Xu, L. Unusual phase behavior of one-component systems with two-scale isotropic interactions. *Journal of Physics: Condensed Matter* **2009**, *21*, 504106.
15. Saija, F.; Prestipino, S.; Malescio, G. Anomalous phase behavior of a soft-repulsive potential with a strictly monotonic force. *Physical Review E* **2009**, *80*, 031502.
16. Malescio, G.; Saija, F. A Criterion for Anomalous Melting in Systems with Isotropic Interactions. *The Journal of Physical Chemistry B* **2011**, *115*, 14091–14098.
17. Prestipino, S.; Saija, F.; Malescio, G. Anomalous phase behavior in a model fluid with only one type of local structure. *Journal of Chemical Physics* **2010**, *133*, 144504.
18. Prestipino, S.; Saija, F.; Giaquinta, P.V. Hexatic phase and water-like anomalies in a two-dimensional fluid of particles with a weakly softened core. *Journal of Chemical Physics* **2012**, *137*, 104503.
19. Coslovich, D.; Ikeda, A. Cluster and reentrant anomalies of nearly Gaussian core particles. *Soft Matter* **2013**, *9*, 6786.
20. Quesada-Perez, M.; Moncho-Jorda, A.; Martinez-Lopez, F.; Hidalgo-Álvarez, R. Probing interaction forces in colloidal monolayers: Inversion of structural data. *Journal of Chemical Physics* **2001**, *115*, 10897.
21. Contreras-Aburto, C.; amd R.C. Priego, J.M. Structure and effective interactions in parallel monolayers of charged spherical colloids. *Journal of Chemical Physics* **2010**, *132*, 174111.
22. Haddadi, S.; Skepö, M.; Jannasch, P.; Manner, S.; Forsman, J. Building polymer-like clusters from colloidal particles with isotropic interactions, in aqueous solution. *Journal of Colloid and Interface Science* **2020**, *581*, 669–681.
23. Grillo, F.; Fernandez-Rodriguez, M.A.; Antonopoulou, M.N.; Gerber, D.; Isa, L. Self-templating assembly of soft microparticles into complex tessellations. *Nature* **2020**, *582*, 219–224. doi:10.1038/s41586-020-2341-6.
24. Ranganathan, V.T.; Bazmi, S.; Wallin, S.; Liu, Y.; Yethiraj, A. Is Ficoll a Colloid or Polymer? A Multitechnique Study of a Prototypical Excluded-Volume Macromolecular Crowder. *Macromolecules* **2022**, *55*, 9103–9112. doi:10.1021/acs.macromol.2c00677.
25. S. Marques, M.; P. O. Nogueira, T.; F. Dillenburg, R.; C. Barbosa, M.; Bordin, J.R. Waterlike anomalies in hard core–soft shell nanoparticles using an effective potential approach: Pinned vs adsorbed polymers. *Journal of Applied Physics* **2020**, *127*, 054701.
26. Lafitte, T.; Kumar, S.K.; Panagiotoulos, A.Z. Self-assembly of polymer-grafted nanoparticles in thin films. *Soft Matter* **2014**, *10*, 786.
27. Bos, I.; van der Scheer, P.; Ellenbroek, W.G.; Sprakel, J. Two-dimensional crystals of star polymers: a tale of tails. *Soft Matter* **2019**, *15*, 615–622.
28. Angell., C.A. Two phases? *Nat. Mater.* **2014**, *13*, 673–675.
29. Gallo, P.; Amann-Winkel, K.; Angell, C.A.; Anisimov, M.A.; Caupin, F.; Chakravarty, C.; Lascaris, E.; Loerting, T.; Panagiotopoulos, A.Z.; Russo, J.; Sellberg, J.A.; Stanley, H.E.; Tanaka, H.; Vega, C.; Xu, L.; Pettersson, L.G.M. Water: A Tale of Two Liquids. *Chemical Reviews* **2016**, *116*, 7463–7500.

30. Gallo, P.; Bachler, J.; Bove, L.E.; Böhmer, R.; Camisasca, G.; Coronas, L.E.; Corti, H.R.; de Almeida Ribeiro, I.; de Koning, M.; Franzese, G.; Fuentes-Landete, V.; Gainaru, C.; Loerting, T.; de Oca, J.M.M.; Poole, P.H.; Rovere, M.; Sciortino, F.; Tonauer, C.M.; Appignanesi , G.A. Advances in the study of supercooled water. *Eur. Phys. J. E* **2021**, *44*, 143.
31. Chaplin, M. Anomalous properties of water. http://www.lsbu.ac.uk/water/anmlies.html, 2023.
32. Kellu, G.S. Density, thermal expansivity, and compressibility of liquid water from 0.deg. to 150.deg.. Correlations and tables for atmospheric pressure and saturation reviewed and expressed on 1968 temperature scale. *J. Chem. Eng. Data* **1975**, *20*, 97–105.
33. Errington, J.R.; Debenedetti, P.D. Relationship between structural order and the anomalies of liquid water. *Nature (London)* **2001**, *409*, 318.
34. Yan, Z.; Buldyrev, S.V.; Giovambattista, N.; Debenedetti, P.G.; Stanley, H.E. Family of tunable spherically symmetric potentials that span the range from hard spheres to waterlike behavior. *Phys. Rev. E* **2006**, *73*, 051204. doi:10.1103/PhysRevE.73.051204.
35. Gibson, H.M.; Wilding, N.B. Metastable liquid-liquid coexistence and density anomalies in a core-softened fluid. *Phys. Rev. E* **2006**, *73*, 061507. doi:10.1103/PhysRevE.73.061507.
36. Vilaseca, P.; Franzese, G. Softness dependence of the anomalies for the continuous shouldered well potential. *The Journal of Chemical Physics* **2010**, *133*, 084507.
37. Xu, L.; Giovambattista, N.; Buldyrev, S.V.; Debenedetti, P.G.; Stanley, H.E. Waterlike glass polyamorphism in a monoatomic isotropic Jagla model. *The Journal of Chemical Physics* **2011**, *134*, 064507, [https://doi.org/10.1063/1.3521486]. doi:10.1063/1.3521486.
38. Reisman, S.; Giovambattista, N. Glass and liquid phase diagram of a polyamorphic monatomic system. *The Journal of Chemical Physics* **2013**, *138*, 064509, [https://doi.org/10.1063/1.4790404]. doi:10.1063/1.4790404.
39. Das, G.; Gnan, N.; Sciortino, F.; Zaccarelli, E. Unveiling the complex glassy dynamics of square shoulder systems: Simulations and theory. *The Journal of Chemical Physics* **2013**, *138*, 134501, [https://doi.org/10.1063/1.4795837]. doi:10.1063/1.4795837.
40. Krott, L.B.; Bordin, J.R.; Barraz, N.M.; Barbosa, M.C. Effects of confinement on anomalies and phase transitions of core-softened fluids. *The Journal of Chemical Physics* **2015**, *142*, 134502, [https://doi.org/10.1063/1.4916563]. doi:10.1063/1.4916563.
41. Luo, J.; Xu, L.; Angell, C.A.; Stanley, H.E.; Buldyrev, S.V. Physics of the Jagla model as the liquid-liquid coexistence line slope varies. *The Journal of Chemical Physics* **2015**, *142*, 224501, [https://doi.org/10.1063/1.4921559]. doi:10.1063/1.4921559.
42. Bordin, J. Waterlike features, liquid-crystal phase and self-assembly in Janus dumbbells. *Physica A: Statistical Mechanics and its Applications* **2016**, *459*, 1–8. cited By 14.
43. Pinheiro, L.; Furlan, A.; Krott, L.; Diehl, A.; Barbosa, M. Critical points, phase transitions and water-like anomalies for an isotropic two length scale potential with increasing attractive well. *Physica A: Statistical Mechanics and its Applications* **2017**, *468*, 866–879.
44. de Haro, M.L.; Rodríguez-Rivas, A.; Yuste, S.B.; Santos, A. Structural properties of the Jagla fluid. *Phys. Rev. E* **2018**, *98*, 012138. doi:10.1103/PhysRevE.98.012138.
45. Higuchi, S.; Kato, D.; Awaji, D.; Kim, K. Connecting thermodynamic and dynamical anomalies of water-like liquid-liquid phase transition in the Fermi–Jagla model. *The Journal of Chemical Physics* **2018**, *148*, 094507, [https://doi.org/10.1063/1.5017105]. doi:10.1063/1.5017105.
46. Ryzhov, V.N.; Tareyeva, E.E.; Fomin, Y.D.; Tsiok, E.N. Complex phase diagrams of systems with isotropic potentials: results of computer simulations. *Physics-Uspekhi* **2020**, *63*, 417. doi:10.3367/UFNe.2018.04.038417.
47. Martín-Roca, J.; Martinez, R.; Martínez-Pedrero, F.; Ramírez, J.; Valeriani, C. Dynamical anomalies and structural features of active Brownian particles characterized by two repulsive length scales. *The Journal of Chemical Physics* **2022**, *156*, 164502, [https://doi.org/10.1063/5.0087601]. doi:10.1063/5.0087601.
48. Bretonnet, J.L.; Bomont, J.M. Analytical treatment of the structure for systems interacting via core-softened potentials. *Chemical Physics* **2022**, *555*, 111445. doi:https://doi.org/10.1016/j.chemphys.2021.111445.
49. Nogueira, T.; Bordin, J.R. Patterns in 2D core-softened systems: From sphere to dumbbell colloids. *Physica A: Statistical Mechanics and its Applications* **2022**, *605*, 128048. doi:https://doi.org/10.1016/j.physa.2022.128048.
50. Bordin, J.R.; Krott, L.B.; Barbosa, M.C. Self-Assembly and Water-like Anomalies in Janus Nanoparticles. *Langmuir* **2015**, *31*, 8577–8582, [https://doi.org/10.1021/acs.langmuir.5b01555]. PMID: 26190234, doi:10.1021/acs.langmuir.5b01555.

51. Bordin, J.R.; Krott, L.B. How Competitive Interactions Affect the Self-Assembly of Confined Janus Dumbbells. *The Journal of Physical Chemistry B* **2017**, *121*, 4308–4317, [https://doi.org/10.1021/acs.jpcb.7b01696]. PMID: 28376295, doi:10.1021/acs.jpcb.7b01696.
52. Jiménez-Millán, S.; García-Alcántara, C.; Ramírez-Hernández, A.; Sambriski, E.; Hernández, S. Self-Aassembly of core-corona colloids under cylindrical confinement: A Monte Carlo study. *Journal of Molecular Liquids* **2021**, *335*, 116219. doi:https://doi.org/10.1016/j.molliq.2021.116219.
53. Pérez-Figueroa, S.E.; Gallegos-Lozano, A.; Mendoza, C.I. Packing core–corona particles on a spherical surface. *Soft Matter* **2022**, *18*, 6812–6824. doi:10.1039/D2SM00719C.
54. Isa, L.; Buttinoni, I.; Fernandez-Rodriguez, M.A.; Vasudevan, S.A. Two-dimensional assemblies of soft repulsive colloids confined at fluid interfaces(a). *Europhysics Letters* **2017**, *119*, 26001. doi:10.1209/0295-5075/119/26001.
55. Wang, J.; Mbah, C.F.; Przybilla, T.; Englisch, S.; Spiecker, E.; Engel, M.; Vogel, N. Free Energy Landscape of Colloidal Clusters in Spherical Confinement. *ACS Nano* **2019**, *13*, 9005–9015, [https://doi.org/10.1021/acsnano.9b03039]. PMID: 31274291, doi:10.1021/acsnano.9b03039.
56. Osterman, N.; Babič, D.; Poberaj, I.; Dobnikar, J.; Ziherl, P. Observation of Condensed Phases of Quasiplanar Core-Softened Colloids. *Phys. Rev. Lett.* **2007**, *99*, 248301. doi:10.1103/PhysRevLett.99.248301.
57. Villada-Balbuena, A.; Jung, G.; Zuccolotto-Bernez, A.B.; Franosch, T.; Egelhaaf, S.U. Layering and packing in confined colloidal suspensions. *Soft Matter* **2022**, *18*, 4699–4714. doi:10.1039/D2SM00412G.
58. Kang, C.; Honciuc, A. Self-Assembly of Janus Nanoparticles into Transformable Suprastructures. *The Journal of Physical Chemistry Letters* **2018**, *9*, 1415–1421, [https://doi.org/10.1021/acs.jpclett.8b00206]. PMID: 29509022, doi:10.1021/acs.jpclett.8b00206.
59. Wu, D.; Honciuc, A. Design of Janus Nanoparticles with pH-Triggered Switchable Amphiphilicity for Interfacial Applications. *ACS Applied Nano Materials* **2018**, *1*, 471–482, [https://doi.org/10.1021/acsanm.7b00356]. doi:10.1021/acsanm.7b00356.
60. Rafael Bordin, J. Distinct self-assembly aggregation patters of nanorods with decorated ends: A simple model study. *Fluid Phase Equilibria* **2019**, *499*, 112251. doi:https://doi.org/10.1016/j.fluid.2019.112251.
61. Bordin, J.R. Distinct aggregation patterns and fluid porous phase in a 2D model for colloids with competitive interactions. *Physica A: Statistical Mechanics and its Applications* **2018**, *495*, 215–224. doi:https://doi.org/10.1016/j.physa.2017.12.090.
62. Cardoso, D.S.; Hernandes, V.F.; Nogueira, T.; Bordin, J.R. Structural behavior of a two length scale core-softened fluid in two dimensions. *Physica A: Statistical Mechanics and its Applications* **2021**, *566*, 125628. doi:https://doi.org/10.1016/j.physa.2020.125628.
63. Fonseca, E.R.; Mendoza, C.I. Self-assembly of core-corona particles confined in a circular box. *Journal of Physics: Condensed Matter* **2019**, *32*, 015101. doi:10.1088/1361-648X/ab42fc.
64. Marques, M.S.; Bordin, J.R. Interplay between adsorption, aggregation and diffusion in confined core-softened colloids. *JCIS Open* **2021**, *4*, 100029. doi:https://doi.org/10.1016/j.jciso.2021.100029.
65. Pekalski, J.; Bildanau, E.; Ciach, A. Self-assembly of spiral patterns in confined systems with competing interactions. *Soft Matter* **2019**, *15*, 7715–7721. doi:10.1039/C9SM01179J.
66. Serna, H.; Noya, E.G.; Góźdź, W.T. Confinement of Colloids with Competing Interactions in Ordered Porous Materials. *The Journal of Physical Chemistry B* **2020**, *124*, 10567–10577, [https://doi.org/10.1021/acs.jpcb.0c08148]. PMID: 33140966, doi:10.1021/acs.jpcb.0c08148.
67. Pant, S.; Ghorai, P.K. Structural anomaly of core-softened fluid confined in single walled carbon nanotube: a molecular dynamics simulation investigation. *Molecular Physics* **2016**, *114*, 1771–1777, [https://doi.org/10.1080/00268976.2016.1149242]. doi:10.1080/00268976.2016.1149242.
68. Bordin, J.R.; Krott, L.B. Confinement effects on the properties of Janus dimers. *Phys. Chem. Chem. Phys.* **2016**, *18*, 28740–28746. doi:10.1039/C6CP05821C.
69. Dobnikar, J.; Fornleitner, J.; Kahl, G. Ground states of model core-softened colloids. *Journal of Physics: Condensed Matter* **2008**, *20*, 494220. doi:10.1088/0953-8984/20/49/494220.
70. Bildanau, E.; Pękalski, J.; Vikhrenko, V.; Ciach, A. Adsorption anomalies in a two-dimensional model of cluster-forming systems. *Phys. Rev. E* **2020**, *101*, 012801. doi:10.1103/PhysRevE.101.012801.

71. Tsiok, E.; Fomin, Y.D.; Ryzhov, V. The effect of confinement on the solid–liquid transition in a core-softened potential system. *Physica A: Statistical Mechanics and its Applications* **2020**, *550*, 124521. doi:https://doi.org/10.1016/j.physa.2020.124521.
72. Fomin, Y.D.; Ryzhov, V.N.; Tsiok, E.N. Interplay between freezing and density anomaly in a confined core-softened fluid. *Molecular Physics* **2020**, *118*, e1718792, [https://doi.org/10.1080/00268976.2020.1718792]. doi:10.1080/00268976.2020.1718792.
73. Fomin, Y.D. Between two and three dimensions: Crystal structures in a slit pore. *Journal of Colloid and Interface Science* **2020**, *580*, 135–145. doi:https://doi.org/10.1016/j.jcis.2020.06.046.
74. Barros de Oliveira, A.; Netz, P.A.; Colla, T.; Barbosa, M.C. Thermodynamic and dynamic anomalies for a three-dimensional isotropic core-softened potential. *The Journal of Chemical Physics* **2006**, *124*, 084505, [https://doi.org/10.1063/1.2168458]. doi:10.1063/1.2168458.
75. de Oliveira, A.B.; Netz, P.A.; Colla, T.; Barbosa, M.C. Structural anomalies for a three dimensional isotropic core-softened potential. *The Journal of Chemical Physics* **2006**, *125*, 124503, [https://doi.org/10.1063/1.2357119]. doi:10.1063/1.2357119.
76. Bordin, J.R.; de Oliveira, A.B.; Diehl, A.; Barbosa, M.C. Diffusion enhancement in core-softened fluid confined in nanotubes. *The Journal of Chemical Physics* **2012**, *137*, 084504, [https://doi.org/10.1063/1.4746748]. doi:10.1063/1.4746748.
77. Krott, L.B.; Barbosa, M.C. Anomalies in a waterlike model confined between plates. *The Journal of Chemical Physics* **2013**, *138*, 084505, [https://doi.org/10.1063/1.4792639]. doi:10.1063/1.4792639.
78. Bordin, J.R.; Diehl, A.; Barbosa, M.C. Relation Between Flow Enhancement Factor and Structure for Core-Softened Fluids Inside Nanotubes. *The Journal of Physical Chemistry B* **2013**, *117*, 7047–7056, [https://doi.org/10.1021/jp402141f]. PMID: 23692639, doi:10.1021/jp402141f.
79. Krott, L.B.; Barbosa, M.C. Model of waterlike fluid under confinement for hydrophobic and hydrophilic particle-plate interaction potentials. *Phys. Rev. E* **2014**, *89*, 012110. doi:10.1103/PhysRevE.89.012110.
80. Krott, L.B.; Bordin, J.R. Distinct dynamical and structural properties of a core-softened fluid when confined between fluctuating and fixed walls. *The Journal of Chemical Physics* **2013**, *139*, 154502, [https://doi.org/10.1063/1.4824860]. doi:10.1063/1.4824860.
81. Bordin, J.R.; Krott, L.B.; Barbosa, M.C. High pressure induced phase transition and superdiffusion in anomalous fluid confined in flexible nanopores. *The Journal of Chemical Physics* **2014**, *141*, 144502, [https://doi.org/10.1063/1.4897956]. doi:10.1063/1.4897956.
82. Bordin, J.R.; Krott, L.B.; Barbosa, M.C. Surface Phase Transition in Anomalous Fluid in Nanoconfinement. *The Journal of Physical Chemistry C* **2014**, *118*, 9497–9506, [https://doi.org/10.1021/jp5010506]. doi:10.1021/jp5010506.
83. Krott, L.B.; Bordin, J.R.; Barbosa, M.C. New Structural Anomaly Induced by Nanoconfinement. *The Journal of Physical Chemistry B* **2015**, *119*, 291–300, [https://doi.org/10.1021/jp510561t]. PMID: 25494049, doi:10.1021/jp510561t.
84. Bordin, J.R.; Barbosa, M.C. Waterlike anomalies in a two-dimensional core-softened potential. *Phys. Rev. E* **2018**, *97*, 022604. doi:10.1103/PhysRevE.97.022604.
85. Dudalov, D.E.; Fomin, Y.D.; Tsiok, E.N.; Ryzhov, V.N. How dimensionality changes the anomalous behavior and melting scenario of a core-softened potential system? *Soft Matter* **2014**, *10*, 4966–4976. doi:10.1039/C4SM00124A.
86. Bordin, J.R.; Krott, L.B. Solid-amorphous transition is related to the waterlike anomalies in a fluid without liquid-liquid phase transition, 2023. doi:10.48550/ARXIV.2302.05999.
87. Allen, P.; Tildesley, D.J. *Computer Simulation of Liquids*; Oxford University Press, Oxford, 1987.
88. Shell, M.S.; Debenedetti, P.G.; Panagiotopoulos, A.Z. Molecular structural order and anomalies in liquid silica. *Phys. Rev. E* **2002**, *66*, 011202. doi:10.1103/PhysRevE.66.011202.
89. Errington, J.R.; Debenedetti, P.D. Relationship between structural order and the anomalies of liquid water. *Nature (London)* **2001**, *409*, 318.
90. Errington, J.E.; Debenedetti, P.G.; Torquato, S. Quantification of Order in the Lennard-Jones System. *J. Chem. Phys.* **2003**, *118*, 2256.

91. Baranyai, A.; Evans, D.J. Direct entropy calculation from computer simulation of liquids. *Physical Review A* **1989**, *40*, 3817 – 3822. Cited by: 357, doi:10.1103/PhysRevA.40.3817.
92. Klumov, B.A.; Khrapak, S.A. Two-body entropy of two-dimensional fluids. *Results in Physics* **2020**, *17*, 103020. doi:https://doi.org/10.1016/j.rinp.2020.103020.